JOURNAL OF MATERIALS SCIENCE 22 (1987) 3173–3177

Characterization of rapidly solidified aluminium–silicon alloy

S. DAS, A. H. YEGNESWARAN, P. K. ROHATGI
Regional Research Laboratory, Council of Scientific and Industrial Research, Hoshangabad Road, Hobibganj Naka, Bhopal 462 026, India

A metallographic investigation of as-cast LM-13 aluminium–silicon alloy, solidified at different cooling rates (using permanent moulds or a single-roll melt spinner), is presented with special reference to the modification of eutectic silicon and the refinement of primary aluminium. The refinement of microstructure with the increase in cooling rate is mainly attributed to the limited growth kinetics of the nucleated phase during solidification. The rapidly solidified ribbon was heat-treated in order to determine the microstructural stability at high temperature. The tensile strength, percentage elongation and hardness values of as-solidified and heat-treated samples correlate well with the changes in the microstructure observed.

1. Introduction

Of all aluminium alloys aluminium–silicon alloys have been studied in detail due to their excellent combination of properties such as fluidity, low coefficient of thermal expansion and high wear resistance. Because of these, Al–Si alloys are finding a large number of applications in the automobile industries, e.g. for pistons, cylinder blocks and liners.

The silicon particles in the aluminium matrix generally grow in the form of needles, platelets or as large cuboids, depending upon the composition of the alloys, leading to an impairment of mechanical and other properties. Thus in order to improve the properties of as-cast alloys, the modification or refinement of silicon is usually done by adding foreign elements or compounds [1–4] to the melt. The growth of silicon can also be controlled by imposing external forces, for instance vibration [5], or by changing the casting conditions, notably by chill casting [6] or by rapid solidification processing. Structural changes through rapid solidification have been of great interest in the last fifteen years [7–18]. Precipitation [7, 10, 15] and kinetics of precipitation [10] of silicon in splat-quenched and melt-spun ribbon have been studied extensively. Previous work on splat-quenched Al–7 wt % Si alloy [19] which was canned and extruded, has shown improvements in yield strength and ductility.

In the present investigation, LM-13 Al–Si alloy has been rapidly solidified and its microstructural features are characterized. Comparison has also been made with the structures obtained at different cooling rates. The mechanical properties of as-solidified and heat-treated samples of rapidly solidified alloy are also reported.

2. Experimental procedure

Al–Si alloy LM-13 (composition: 11 to 13 wt % Si, 1 wt % Cu, 1.5 wt % Ni, 0.5 wt % Fe, 0.5 wt % Mn and the rest aluminium) was rapidly solidified from the melt using a single-roll melt-spinning unit. The melt impinged on the substrate, flattened and solidified as a ribbon. The details of the process are given elsewhere [20]. The ribbon was 42 mm wide and its thickness varied from 180 to 220 μm. In addition, LM-13 alloy melt was cast in a rectangular mould of size 40 mm × 14 mm × 20 mm and in a cast-iron mould of 18 mm internal diameter. For metallographic observation samples were cold-mounted, mechanically polished, etched with Keller's reagent and observed by optical and scanning electron microscopy (SEM). The silicon particle size and secondary dendrite arm spacing were measured using quantitative metallographic techniques. For SEM observation, samples were deeply etched and coated with a thin layer of silver to avoid the charging effect. X-ray diffraction analysis was carried out using Cu$K\alpha$ radiation with a view to identifying the elements present in the rapidly solidified ribbon. Tensile samples of 25 mm gauge length were prepared from the rapidly solidified ribbons and tested in an Instron machine with a cross-head speed of 2 mm min^{-1}. The load–elongation values were recorded from the chart. Microhardness measurements were performed on the metallographically prepared samples using a load of 10 Pa. At least five readings were taken on each sample and the average value with the scatter was plotted.

3. Results and discussion

Metallographic examination of the solidification structure of as-cast LM-13 alloy, cast in a cast-iron mould, shows α-aluminium dendrites with eutectic silicon in the interdendritic region. The average dendrite arm spacing (DAS), i.e. centre-to-centre distance between two neighbouring dendrites, was found to be $\sim 12\,\mu$m. It is generally known that the eutectic silicon grows anisotropically by a twin-plane re-entrant edge mechanism (TPRE) in the $\langle 2\,1\,1\rangle$ direction, growing straight for some distance and then branching off or changing its direction through a large angle by multiple twinning [21]. Figs 1 and 2 show the optical and SEM

0022–2461/87 $03.00 + .12

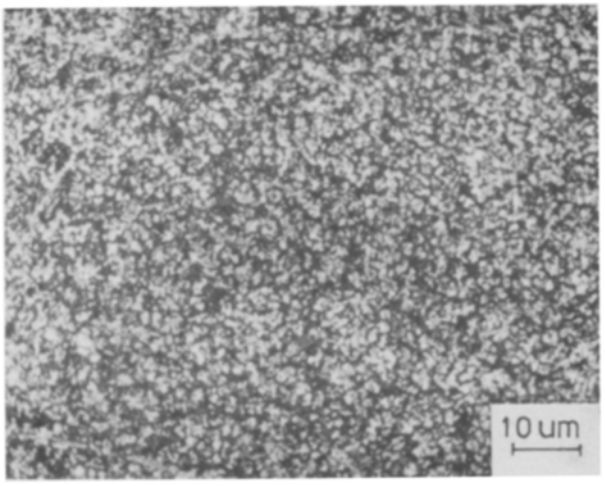

Figure 1 Optical micrograph of melt-spun ribbon.

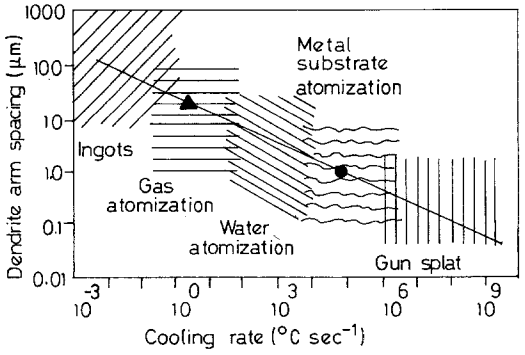

Figure 3 Dendrite arm spacing as a function of cooling rate for aluminium and aluminium alloys: (●) rapidly solidified LM-13, (▲) permanent-mould cast (cast-iron).

micrographs, respectively, of melt-spun ribbon. Optical micrograph shows very fine α-aluminium dendrites (DAS = 1 μm) and eutectic silicon in the interdendritic region (black patches), which is clearly revealed in an SEM micrograph, Fig. 2. X-ray diffraction studies of this microstructure show sharp peaks corresponding to (1 1 1) and (2 2 0) planes of silicon and (1 1 1) of aluminium; other elements present in LM-13 alloy, e.g. copper, magnesium and nickel, have not been detected by X-ray analysis. This may be because these alloying elements, which are present in small quantities below 2%, have gone into the solid solution due to rapid solidification processing.

The cooling rates of as-solidified alloys were estimated from the master diagram, Fig. 3, correlating the dendrite arm spacing and cooling rate for aluminium and its alloys [22, 23]. In the present case the cooling rates were of the order of 10^5(° C) sec^{-1} in the rapidly solidified ribbons and 10(° C) sec^{-1} in the permanent-mould castings.

Another notable effect of rapid solidification, as seen in Fig. 2, is the change in the growth morphology of eutectic silicon to a more or less spheroidal shape, from the plate-like shape as observed in permanent-mould casting. The size of silicon was found to be of the order of 1 μm. Fig. 4 shows an SEM micrograph of LM-13 alloy cast in a copper mould of sample thickness 1 mm. This figure clearly reveals the semi-isotropic growth of silicon crystals in the aluminium matrix. With a further increase in the casting thickness to 5 mm (decrease in cooling rate) the structure, as seen in Fig. 5, shows branched fibrous eutectic silicon. Hence the most significant structural changes as a result of rapid solidification are a decrease in the secondary dendrite arm spacing of the primary aluminium phase and a change in the morphology of eutectic silicon.

The refinement of primary aluminium dendrites depends on how fast the heat can be dissipated from the melt during solidification, so that after nucleation there is less time available for growth of the nucleated phase. In rapid quenching, the alloy melt is generally undercooled to a temperature well below the solidus line, and nucleation begins essentially at a lower temperature. This results in an increase of nucleation events, and rapid extraction of heat from the melt reduces the time available for growth thereby restricting the growth of the nucleated phase. However, the alteration of growth morphology of silicon crystals from anisotropic (solidification in cast-iron mould) to more or less isotropic (rapid rate of solidification) may be attributed to a transition from a faceted to a non-faceted growth mode. Generally, faceted and non-faceted growths are dictated by the Jackson α-factor

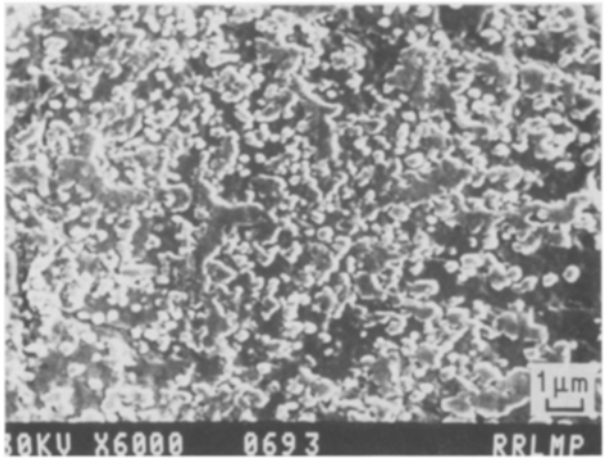

Figure 2 SEM micrograph, showing modified eutectic silicon after rapid solidification processing.

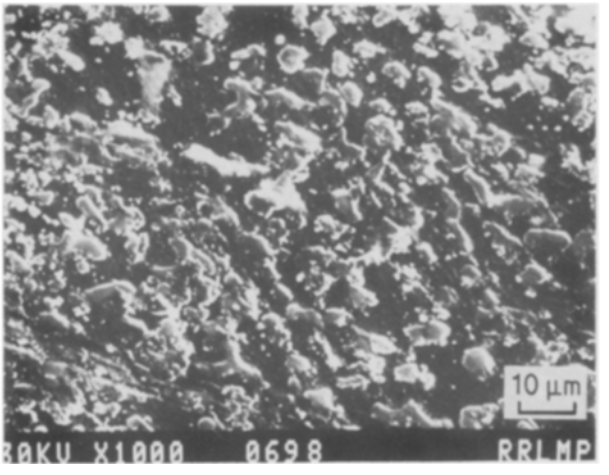

Figure 4 SEM micrograph of LM-13 alloy cast in a copper mould (sample thickness 1 mm).

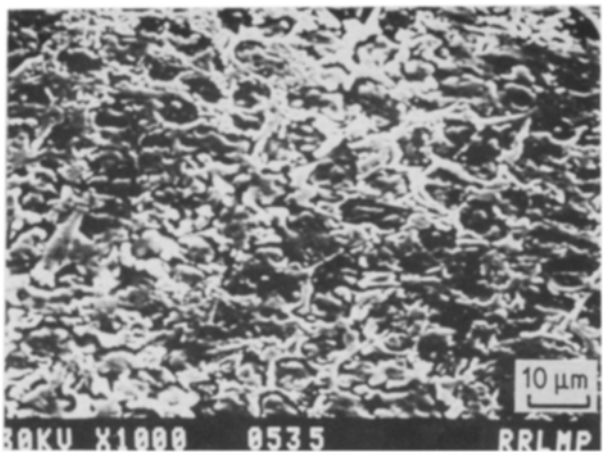

Figure 5 SEM micrograph of LM-13 alloy cast in a copper mould (sample thickness 5 mm).

[24], and silicon occupies an intermediate value of $\alpha = 2$ to 5. It is suggested that as undercooling during solidification increases, the anisotropy of growth rate between different crystallographic directions decreases. It has been observed in the present study that when LM-13 alloy is solidified in a copper mould of sample thickness 1 mm and 5 mm, where the solidification rate is lower than in the melt-spun ribbon, the silicon crystals grow as semi-isotropic and fibrous, respectively. It is reasonable to conjecture from the above facts that the faceting tendency of silicon could be reduced by increasing the cooling rate and consequently the undercooling.

The mechanical properties of the rapidly solidified LM-13 alloy after heat treatment mainly depend on the microstructural stability. To make an assessment, melt-spun LM-13 alloy ribbon was annealed at different temperatures for 1 h. The structures were examined under an optical microscope at room temperature. Figs 6a to c show the microstructures of rapidly solidified LM-13 alloy ribbon aged at 525, 625 and 725 K for 1 h. It is seen that a coarsening of second-phase silicon particles occurs with the increase in annealing temperature. In order to gain further information on the coarsening tendency of the eutectic silicon one sample was annealed at 725 K for 17 h (Fig. 6d). The microstructure clearly reveals silicon particles in spherical form and randomly distributed in the aluminium matrix. The silicon particles were found to be of 3 to 5 µm size. The interparticles spacing is shown in the form of a histogram in Fig. 7.

Fig. 8 shows the ultimate tensile strength and elongation of as-rapidly-solidified and heat-treated LM-13 alloy. For comparison the strength and elongation of LM-13 alloy cast in permanent moulds are also included. It is seen that the strength of rapidly solidified alloy has increased to 260 MPa from that of 180 MPa for cast alloy. The ductility has also increased. The improvement in strength and ductility is mainly attributed to (a) a decrease in inter-

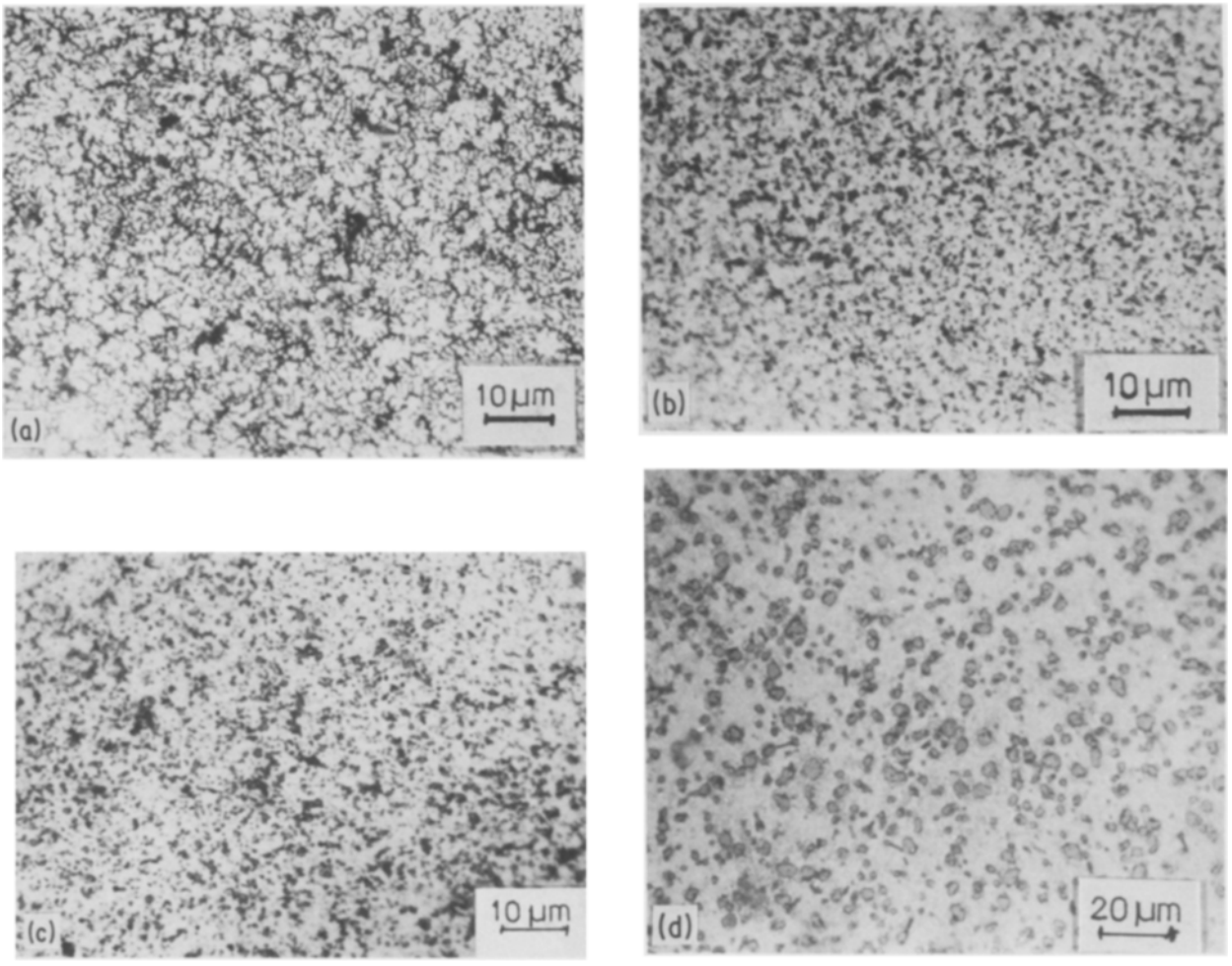

Figure 6 Microstructure of heat-treated rapidly solidified LM-13 alloy: (a) 525 K, 1 h; (b) 625 K, 1 h; (c) 725 K, 1 h; (d) 725 K, 17 h.

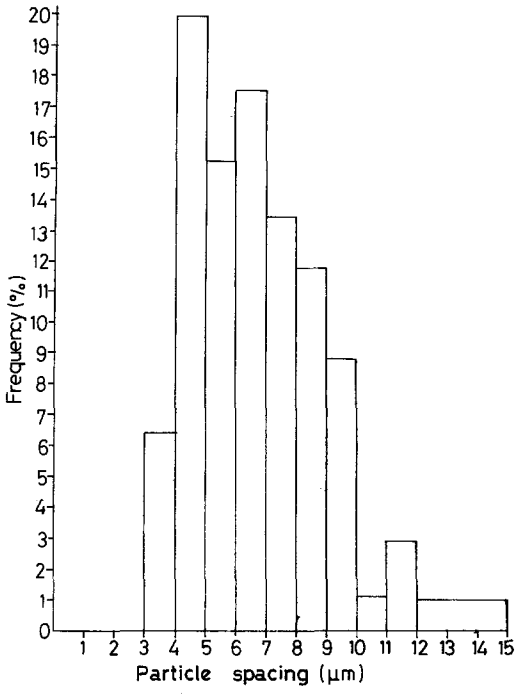

Figure 7 Frequency distribution of interparticle spacing (annealed for 17 h at 723 K).

dendritic spacing and (b) a modification of the silicon morphology.

The decrease in strength of rapidly solidified alloy with increase in the annealing temperature, as seen in Fig. 8 is mainly due to the coarsening of silicon particles. This effect is conspicuous in the samples that had been annealed for 17 h at 723 K (Fig. 6d). The variation in microhardness with annealing temperature, shown in Fig. 9, also behaves in the same way as the strength. Thus the decrease in strength and hardness of rapidly solidified LM-13 alloy with temperature is mainly attributed to a coarsening of the microstructure.

4. Conclusions

1. LM-13 alloy was rapidly solidified from the melt in the form of a ribbon at a cooling rate of about 10^5(° C) sec^{-1}.

2. The secondary dendrite arm spacing of the aluminium phase in the rapidly solidified structure was found to be of the order of 1 μm. Scanning electron microscopy reveals that the growth morphology of eutectic silicon has changed from plate-like in conventional die casting to spheroidal by rapid solidification processing.

Figure 8 (○) Ultimate tensile strength and (■) elongation with increasing annealing temperature of rapidly solidified LM-13 alloy; (●) elongation and (△) UTS for samples cast in a permanent mould.

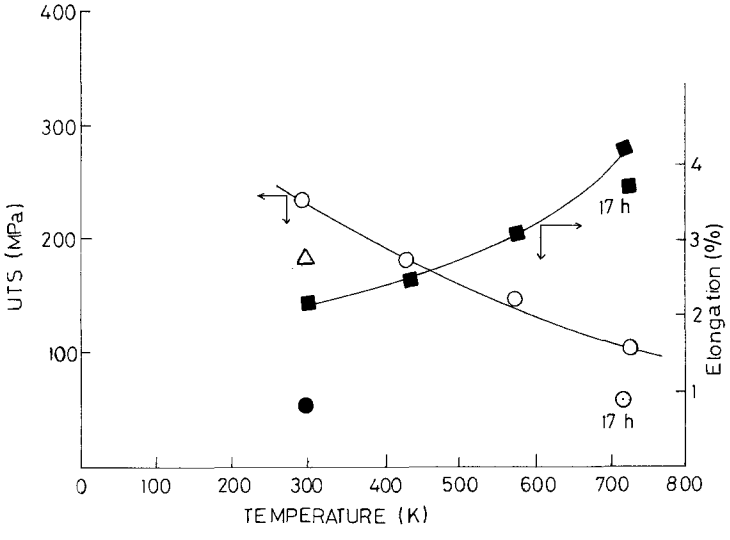

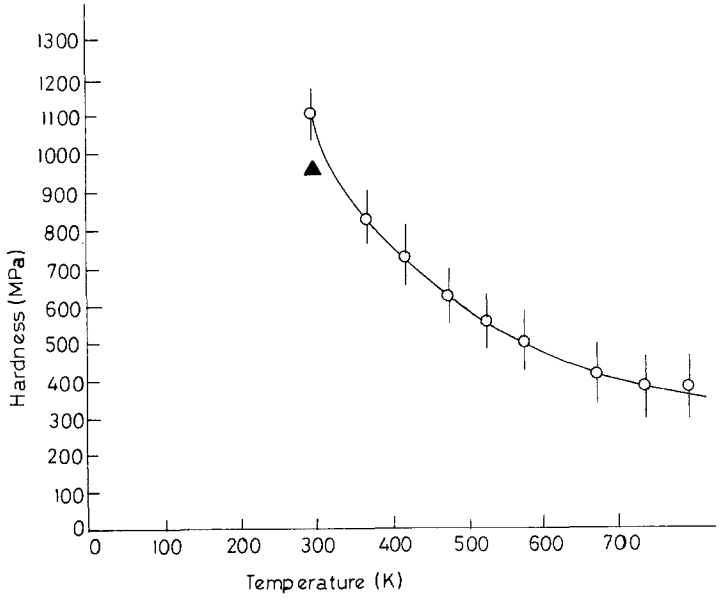

Figure 9 Microhardness values with increasing annealing temperature of rapidly solidified LM-13 alloy; (▲) permanent-mould cast.

3. The rapidly solidified alloy shows improvements in tensile strength, ductility and hardness compared to the alloy cast in a permanent mould. This is mainly attributed to the refinement of the microstructure.

4. The coarsening of the structure has occurred as a result of ageing, and this resulted in a decrease in the tensile strength and hardness.

Acknowledgements

The authors wish to thank Dr J. A. Sekhar, Scientist, DMRL, Hyderabad, for extending facilities for melt-spinning. Thanks are also due to Professor T. R. Ramachandran of IIT, Kanpur, for X-ray diffraction studies. The authors also wish to thank Mr K. K. S. Gautam and Dr S. V. Prasad for their technical assistance in SEM.

References

1. A. PACZ, US Patent 1 387 900 (1921).
2. A. HELLAWELL, *Prog. Mater. Sci.* **15** (1970) 1.
3. W. KURZ and D. J. FISHER, *Int. Met. Rev.* **244** (1979) 177.
4. M. D. HANNA, SHU-ZU LU and A. HELLAWELL, *Met. Trans.* **15A** (1984) 459.
5. G. S. COLE and G. F. BOLLING, *Trans. Met. Soc. AIME* **239** (1967) 1824.
6. Y. TSUMURA, *Nippon Kinzoku Gakkai-Shi* **21** (1957) 69.
7. M. ITAGAKI, B. C. GIESSEN and N. J. GRANT, *Trans. Amer. Soc. Met.* **61** (1968) 330.
8. S. K. BOSE and R. KUMAR, *J. Mater. Sci.* **8** (1973) 1795.
9. S. C. AGARWAL, M. J. KOCZAK and H. HERMAN, *Scripta Metall.* **7** (1973) 365.
10. H. MATYJA, K. C. RUSSELL, B. C. GIESSEN and N. J. GRANT, *Met. Trans.* **6A** (1975) 2249.
11. A. BENDIJK, R. DELHEZ, L. KATGERMAN, TH. H. DE KEIJSER, E. J. MITTEMEIJER and N. M. VAN-DERPERS, *J. Mater. Sci.* **15** (1980) 2803.
12. E. J. MITTEMEIJER, P. VAN MOURIK and TH. H. DE KEIJSER, *Acta Crystallogr. (Suppl.)* **(A) 37** (1981) C-153.
13. R. DELHEZ, TH. H. DE KEIJSER, E. J. MITTEMEIJER, P. VAN MOURIK, N. M. VANDER PERS, L. KARGERMAN and W. E. ZALM, *J. Mater. Sci.* **17** (1982) 2887.
14. J. A. VAN DER HOEVEN, P. VAN MOURIK and E. J. MITTEMEIJER, *J. Mater. Sci. Lett.* **2** (1983) 158.
15. P. VAN MOURIK, E. J. MITTEMEIJER and TH. H. DE KEIJSER, *J. Mater. Sci.* **18** (1983) 2706.
16. V. I. DOBATKIN, V. V. GOLDEV and V. V. BELOTSERKOVETS, Nauka 11764, G.S.P-7, Moscow, V-485; Profsoyuznaya ul. 90, USSR, 1982, *Metalurgiya i Metalovedenie Tsvetynykh Splavov* (53-60).
17. P. H. SHINGU, K. KOBAYASHI, K. SHIMOMURA and R. OZAKI, *Nippon Kinzoku Gakkaishi* **37** (4) (1973) 433.
18. K. N. ISHIHARA and P. H. SHINGU, *J. Mater. Sci. Lett.* **3** (1984) 1015.
19. N. J. GRANT, "High Temperature Materials Phenomena", in Proceedings of 3rd Nordic High Temperature Symposium (1972) edited by J. Rasmussen (Polyteknik Forlag, Denmark, 1973) p. 10.
20. H. H. LIEBERMANN and C. D. GRAHAM, *IEEE Trans. Magn.* **MAG 12** (1976) 921.
21. K. F. KOBAYASHI and L. M. HOGAN, *J. Mater. Sci.* **20** (1985) 1961.
22. W. A. DEAN and R. E. SPEAR, in Proceedings of 12th Army Materials Research Conference, edited by J. J. Burke, N. L. Reed and V. Weiss (Syracus University Press Syracuse, New York, 1966) p. 268.
23. H. MATYJA, B. C. GIESSEN and N. J. GRANT, *J. Inst. Met.* **96** (1968) 30.
24. K. A. JACKSON, "Liquid metals and solidification" (American Society for Metals, Cleveland, Ohio, 1958) p. 174.

Received 17 March
and accepted 4 September 1986